Comparison of Hybrid-III and PMHS Response to Simulated Underbody Blast Loading Conditions

Ann M. Bailey, John J. Christopher, Kyvory Henderson, Fred Brozoski, Robert S. Salzar

Abstract Military vehicle underbody blast is the cause of many serious injuries in theatre today. The purpose of this research was to determine the loading conditions relevant to underbody blast which would produce characteristic lower extremity and pelvis injuries. In addition to better understanding the response of the human to high rate vertical loading, this test series also aimed to supplement the available information on the response of the Hybrid-III under such loading conditions. Five full body matched pair post mortem human specimen (PMHS) and Hybrid-III anthropometric test device (ATD) tests were completed using the University of Virginia's ODYSSEY simulated blast rig under a range of loading conditions. Seat pan loading accelerations ranged from 291 to 738 g's over three milliseconds and foot pan accelerations from 234 to 615 g's over three milliseconds. Post-test CT scans and necropsies were performed to determine any injuries, and revealed a combination of pelvic, lumbar, thoracic, and lower extremity injuries. This research demonstrates the inaccuracy of the Hybrid-III under high rate vertical loads as well as preliminarily suggest the vertical injury threshold for the pelvis exists around 300g's of acceleration and 6.5 m/s peak velocity in 5 ms, while the threshold for the lower extremities lies in excess of 600 g's of acceleration and 10 m/s peak velocity in 4.5 ms.

Keywords Hybrid-III, injury, lower extremity, Mil-LX, underbody blast

I. INTRODUCTION

Severe injuries are being reported from occupants of military vehicles exposed to under-body blasts, with lower extremity and pelvic injuries accounting for a significant portion of these injuries. However, both the etiology of these injuries and an effective means to mitigate these injuries are not currently known or understood, although whole body accelerations and at least some limited toe-pan intrusion are expected. Furthermore, there is currently no objective test methodology to determine the risk of injury to the lower extremities due to foot-well intrusion or pelvic injury due to seat pan translation from an under-vehicle blast. While other serious injuries may accompany pelvis and lower extremity injuries in an underbody blast (UBB) event, the direct loading of both the lower extremities and the pelvis make them a key starting point for investigating the injury mechanisms of UBB. Additionally, the ability to evacuate the vehicle following a UBB event in order to avoid further threat by the enemy in live theater makes the prevention of both lower extremity and pelvic injuries a top priority because of their weight-bearing nature and necessity for walking.

Lower extremity injuries are some of the most frequent, severe and debilitating injuries generated by underbody blast. Lower limb injuries sustained in automobile crashes have been heavily researched due to their frequency and high likelihood of impairment and disability. A review of the literature suggests that lower limb injuries account for roughly one-third of all moderate-to-serious injuries sustained by motor vehicle occupants involved in frontal crashes [1-3]. Since intrusion of the foot-well region is often postulated as the primary mechanism of below-knee lower limb injuries, intrusion characteristics such as toe-pan displacement, toe-pan acceleration, intrusion onset rate, intrusion duration, and intrusion initiation time have been examined for their potential to produce lower limb trauma.

The injury mechanisms of the lower limb associated with intrusion of the foot include inertial loading, entrapment, excessive motion of the joints, and subsequent contact with other structures within the occupant compartment [4]. In terms of mechanisms associated with these injuries, the most severe trauma is normally sustained from axial loading of the limb. Biomechanical testing has been conducted to develop basic injury

*A.M Bailey is a Ph.D. student in mechanical engineering at the University of Virginia in Charlottesville, VA (434-296-7288 (phone), 434-296-3453 (fax), amb9um@virginia.edu). J.J. Christopher is a M.S. student in mechanical engineering at the University of Virginia in Charlottesville, VA. K. Henderson is a B.S. of mechanical engineering and currently works at the University of Virginia in Charlottesville, VA. F. Brozoski works for the U.S. Army Aeromedical Research Lab in Fort Rucker, Alabama. R.S. Salzar is a Ph.D. of mechanical engineering and currently works at the Center for Applied Biomechanics at the University of Virginia.

criteria for axial loading of the below-knee structures. For automotive rates of loading, Yoganandan et al. conducted a series of axial impact tests to the human foot-ankle complex and found a mean dynamic force at fracture (calcaneus and distal tibia) to be 15.1 kN [5]. Funk et al. (2002) determined injury risk functions for axial loads to the foot/ankle complex from a study that included axial loads up to approximately 12 kN [6].

The appropriateness of automotive rate tests for UBB applications can be understood by examining the different resulting injuries in each type of event. For example, in Funk et al., 2002, a test series investigating automotive intrusion produced averaged toe-pan velocities of 5 m/s with a load duration of 10ms (approximately 50g, compared to estimates of UBB accelerations of 500+g) [6]. In that study of 43 specimens, this load rate produced 9 talus, 25 calcaneus, 7 pilon, 4 medial malleolus, 8 lateral malleolus, 2 fibula, and 12 tibial plateau fractures. In 2001, Wang reported that underbody blasts can produce accelerations averaging 100g over time spans of 3 to 100 ms [7]. For most tests performed, the acceleration is not reported. Others have reported floor plate velocities produced by mine blasts to reach up to 30 m/s in 6 to 10 ms [8]. A study performed by McKay at loading velocities of 7, 10 and 12 m/s produced injuries similar to the Funk study in 2002; however, each of the tests performed at 10 m/s and above produced calcaneus injuries, with the talus being the second most injured bone. McKay concluded that severity of injury to the tibia and fibula increased with increasing impact velocities, thus suggesting that automotive rate loading is insufficient for determining injury thresholds for UBB [9]. A summary of previous lower extremity tests with sufficient detail for cross-comparison is shown in TABLE 1.

TABLE 1

SUMMARY OF PREVIOUS LOWER EXTREMITY UBB RESEARCH

Study	Boundary Condition	Hammer Mass (kg)	Velocity (m/s)	Max Energy (J)	Force (kN)	Acceleration (G)
Schueler 1995 [10]	Whole body	38	12.5	2968.8	16	250
McKay 2009 [11]	Femur potted	36.7	7.2-11.8	941-2494	4-6	Unreported
Yoganandan 1996 [12]	Ballast 16.8kg	25	7.6	722	4.3-11.4	Unreported
Kitagawa 1998 [13]	Fixed end	18	3.99	143.3	7-9	Unreported
Quenneville 2010 [14]	Free end	3.9	13.9	109.6	15	Unreported
Bass 2004 [15]	Free end	N/A	Unreported	200g of C4	>8.6	25-200

As evidenced by TABLE 1, a reasonable amount of research has attempted to focus on the effect of UBB load rates on the lower extremities. However, practically all of the biomechanical research on the pelvis has been conducted under automotive type loading. Near-side automotive impacts (where the incoming vehicle strikes the target vehicle side) are the number one cause of pelvic injuries [16-[**17**]. Side impacts tend to produce lateral compression fractures on the pelvic ring that involve the pubic rami, sacrum and iliac wing. In a clinical study on pelvic injuries in side impacts, States and States (1968) found predominantly pubic rami fractures and sacral crush [18]. Acetabular fractures with central dislocation of the femoral head were noted among a small percentage of side impact victims. Grattan and Hobbs (1969) studied hip joint injuries in side impacts and also found predominantly pubic rami fractures, along with some centrally dislocated acetabular fractures [19]. Other clinical data indicate that acetabular fractures do occur in automotive side impacts [20-21]. Salzar, et al. (2009) found that pelvic fracture could be predicted by prescribing the height of the intruding structures, allowing either acetabulum, pubic rami and pubic symphysis fractures if impacted low on the pelvis, or sacroiliac (SI) joint fracture if impacted higher on the pelvis [22]. Gokcen et al. (1994), in a surveillance study of pelvic fractures resulting from car crashes, found a mortality rate of roughly 50% and unsatisfactory treatment among one-third of the survivors [16]. Guillemot et al. (1997) found that near-side impacts account for 94% of the sacroiliac joint injuries. Under very high energy impacts, an unstable fracture of the pelvis such as open book pelvic fractures usually occurs, with failure of the SI ligaments [23]. So far, little information is available about the injury mechanisms of the SI joint in automotive collisions, and the role of accessory ligaments on the SI joint stability and mobility is still not well understood.

Salzar et al. (2006) developed a femur-loaded, position-dependent injury tolerance of the pelvis for a frontal impact direction. This study found an axial injury tolerance based on peak force to be 6,850N for the extended, neutral seated position, and 4,090N in the flexed, neutral position. From the flexed neutral orientation, the peak axial force increased 18% for 20° abduction and decreased 6% for 20° adduction [24]. This variation in fracture tolerance due to femur position indicates the need for further refinement of pelvic injury criteria.

An overarching observation from the available literature on pelvis injury is that there is significant correlation between direction of impact and injury pattern, which further stresses the need to investigate the response of the pelvis under UBB specific loads [25-27]. The injuries commonly produced in UBB events, such as pelvic ring and ischium fractures are not commonly associated with automotive-type loading; thus it is important to reproduce these fractures in a controlled UBB-like environment to fully understand the mechanisms of pelvis injury associated with UBB.

While a lot of biomechanical knowledge already exists for the lower extremities and pelvis, much of the data are limited to automotive rates, meaning the data possess several critical limitations for use in the development of injury countermeasures in the under-body blast environment: these tests have not been developed for rates of loading indicative of the vehicle-blast environment; and they have not included relevant attire (such as combat boots or personal protective equipment). The applicability of these studies and criteria remain a key question to answer in the course of this study. Additionally, while anti-personnel landmine blast studies such as Bass, et al. in 2004 performed tests on PMHS and surrogate limbs exposed to C4 landmine blasts, the loading conditions are not as well defined as an impact test so the results are difficult to compare to UBB conditions and do not provide insight into the response of the whole body. Characterization of how the higher loading rates of UBB affect the response of the lower limb and pelvis will provide valuable information towards understanding the relevant injury mechanisms in UBB events, and is essential in the process of developing a biofidelic anthropomorphic test device (ATD). There is currently no objective test methodology to determine the transmission of forces, nor the risk of injury to the lower extremities due to foot-well intrusion from an under-vehicle blast or to the pelvis due to vertical translation of the seat. This research investigates injury and response of vehicle occupants (both PMHS and ATD) subjected to under body blast (UBB). In order to understand the mechanisms of injury resulting from UBB, laboratory experiments must be performed that recreate the blast-induced intrusion and motion of the vehicle, allow full visualization of the impact event, and include detailed instrumentation of the Post-Mortem-Human-Specimens (PMHS), crash test dummies and vehicle. This paper details a first attempt at whole body testing for a lab-based UBB scenario, while comparing the response of both PMHS and ATD occupants under these high rate loads in matched-pair tests, with particular attention to the lower extremities and pelvis.

II. METHODS

Using the University of Virginia's ODYSSEY blast rig, five whole body postmortem human surrogate (PMHS) tests were performed with matched pair Hybrid-III anthropomorphic test dummy (ATD) tests (TABLE 2). PMHS were obtained for this testing through the Virginia State Anatomical Board and other tissue suppliers accredited by the American Association of Tissue Banks. The test protocols were subject to review by the University of Virginia Cadaver Use Committee.

TABLE 2
PMHS SPECIMEN INFORMATION

Specimen	Age (years)	Weight (lb)	Stature	Cause of Death
566	61	223	5'11"	Respiratory Failure
567	67	180	5'11"	Cardiopulmonary Arrest
526	59	225	6'0"	Melanoma
569	66	230	5'8"	COPD
520	65	155	5'8"	Cardiopulmonary arrest and myocardial infarction

ODYSSEY Blast Rig

The ODYSSEY blast rig consists of two independent sleds mounted to a Via Systems Model 713 sled track. The hammer sled (Fig. 1) consists of a frame on which two sliding hammers are mounted. The hammer weights are adjustable to change the energy input conditions of the test as well as to compensate for heavier or lighter test specimens to ensure proper energy management. The hammer positions may be adjusted to produce a timing delay in the seat and foot pan pulses. The speed of the hammer sled is controlled by a pressurized cylinder system, and blocks of polyurethane are used to shape the input acceleration pulses on both the seat and foot platens.

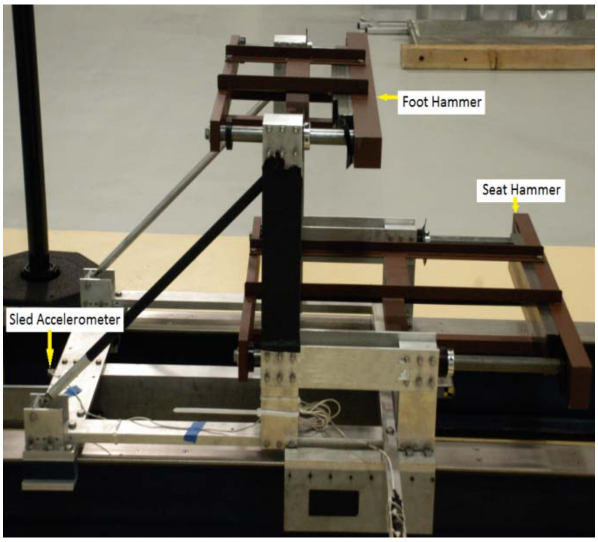

Fig. 1. Hammer Sled

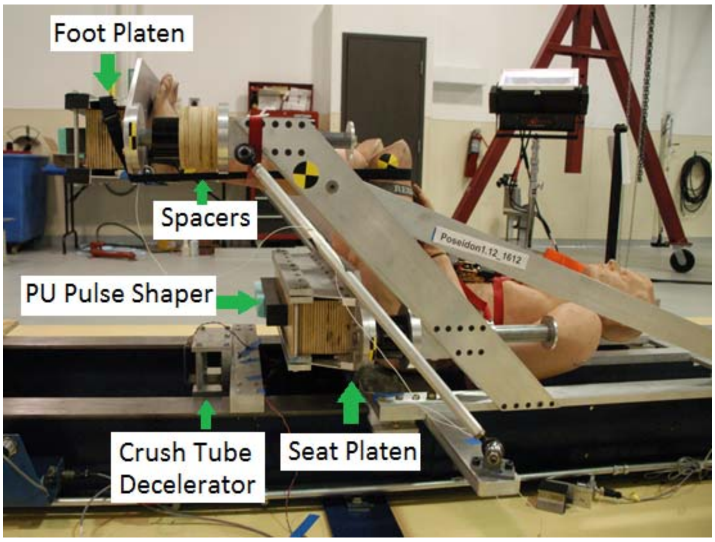

Fig. 2. Carriage sled and crush-tube decelerator assembly

The second sled, the carriage sled (Fig. 2) uses the rails of the track for stability, but does not use the sled's powering mechanism. This sled holds the test specimen and contains both seat and foot platens that the hammers impact. The carriage sled is placed a specified distance from the launch end of the sled rails to allow for enough run-up distance for the hammer sled. The carriage sled shoe compression is adjustable in order to control the post-impact carriage sled movement. The seat and foot platens are attached to the carriage sled using sliding shafts which are adjusted to control the stroke of each platen. Polyurethane spacers are positioned around each of the sliding shafts which create a braking pulse for the platens and allow for separation of the foot and seat platens from the test subject after the initial impact occurs. Spacers can also be placed on the sliding shafts to accommodate differences in specimen anthropometry as well as to adjust the knee-thigh-hip angles for studying the effects of different seated postures.

Another key component to the ODYSSEY blast rig is the crush-tube decelerator. This decelerator slows the mass of the hammer sled frame and allows only the mass of the two hammers to contribute to the impact event. The decelerator consists of a frame, which is bolted to the sled tracks and holds a piece of square steel tubing. A six-inch wide snoot attached to the front of the hammer sled impacts the side of the tubing and crushes the tube at a rate dependent upon the yield strength of the steel. By manipulating the length of the tubing, the deceleration of the hammer sled can be controlled to regulate the stresses on the hammer sled and to allow for travel of the foot and seat hammers.

Data Acquisition and Instrumentation

The five whole body PMHS tests were performed in order to find thresholds of injury for underbody-blast loading conditions. The main regions of interest were the pelvis and the lower extremities, because of their proximity to the loading points; however, other key body regions were instrumented in order to determine the transmissibility of loads in the human body in comparison to the ATD. A summary of the input parameters for the five Hybrid-III tests can be found in Table 4. Each test was performed with the specimen wearing Belleville (Belleville Boot Company, Belleville, IL) Lightweight Desert Combat Boots and a 5-point harness restraint.

Table 3
PMHS TEST MATRIX

Test	Specimen	Velocity (m/s)	Foot Hammer Mass (kg)	Seat Hammer Mass (kg)	Max Foot Acceleration (g) in (ms)	Max Seat Acceleration (g) in (ms)	Foot-Tibia-Femur Angles (Deg)
1.1	566	14.167	32.44	68.605	614.8 in 1.05	737.9 in 2.96	90-90
1.2	567	13.56	32.44	68.605	585.3 in 1.25	734.9 in 2.96	90-90
1.3	526	7.59	32.44	68.605	233.9 in 2.17	291.2 in 4.54	90-90
1.4	569	8.99	32.44	57.107	304.9 in 1.91	326.2 in 4.54	90-90
1.5	520	12.96	32.44	68.605	686.4 in 1.19	309.3 in 6.45	90-90

TABLE 4
HYBRID III TEST MATRIX

Test	Velocity (m/s)	Foot Hammer Mass (kg)	Seat Hammer Mass (kg)	Max Foot Acceleration (g) in (ms)	Max Seat Acceleration (g) in (ms)	Foot-Tibia-Femur Angles (Deg)
2.1	13.98	32.44	68.605	516.7 in 1.26	918.7 in 1.91	90-90
2.2	13.98	32.44	68.605	565.4 in 1.22	701.2 in 3.22	90-90
2.3	8.09	32.44	68.605	278.0 in 2.11	356.4 in 5.33	90-90
2.4	8.87	32.44	57.107	330.4 in 1.97	323.2 in 4.48	90-90
2.5	13.13	32.44	68.605	530.3 in 1.36	421.4 in 2.78	90-90

Table 3 shows the test conditions for the PMHS tests, while Table 4 shows the conditions used for the ATD tests which were purposefully chosen to match the conditions from the PMHS tests. The relative seat and foot platen loading conditions were chosen to narrow in on injury thresholds rather than mimic UBB conditions. However, the input velocities are characteristic of those observed in UBB events [7]. Cadaveric specimens were instrumented with a more rigorous instrumentation outfit, which concentrated on the lower extremities (Table 5). The lower extremity instrumentation consisted of fifteen total strain gages (CEA 06-062UW-350/P2, Micro-Measurements, Raleigh, NC) attached along the tibia and femur diaphysis and calcanei to capture strains in the SAE-Z direction using cyanoacrylate adhesive (Fig. 4). Additionally, the left and right, 4^{th} and 8^{th} ribs were instrumented with strain gages as well as key positions on the pelvis. Six-degree-of-freedom accelerometer cubes were attached to each distal tibia and distal femur using a nonintrusive worm drive hose clamp design. Additional accelerometer cubes were attached to the temporal bone on the left side of the head, the posterior sacrum, T1 vertebrae and the anterior sternum using wood screws. These cubes contained accelerometers positioned in the SAE-X and SAE-Z directions, and an angular rate sensor positioned in the SAE-Y direction. Combinations of Endevco 7264B-2k and 7270A-6000 accelerometers and ARS -12k and -18k angular rate sensors were used to instrument these cubes.

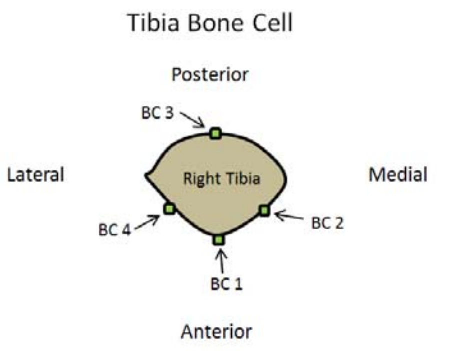

Fig. 3. Tibia strain gage array configuration

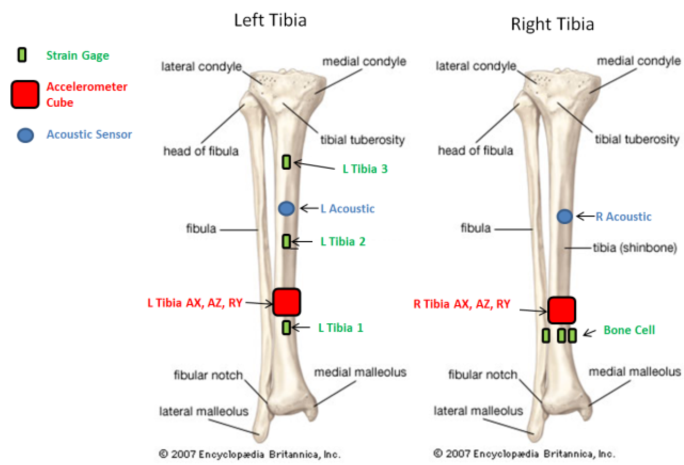

Fig. 4. Tibia instrumentation

TABLE 5
PMHS INSTRUMENTATION LIST

Measurement	Instrument	Sampling Rate
T1 and Pelvis Acceleration SAE-X, Z	Endevco 7264B-2000	1 MHz
T1 and Pelvis Angular Rate SAE-Y	DTS ARS-12k	1 MHz
Sternum Acceleration SAE-X, Z	Endevco 7264B-2000	1 MHz
Right and Left Tibia Acceleration SAE-X	Endevco 7264B-2000	1 MHz
Right and Left Tibia Acceleration SAE-Z	Endevco 7270A-6000	1 MHz
Right and Left Tibia Angular Rate SAE-Y	DTS ARS-18k	1 MHz
Right and Left Femur Acceleration SAE-X, Z	Endevco 7264B-2000	1 MHz
Right and Left Femur Angular Rate SAE-Y	DTS ARS-18k	1 MHz

Right and Left Tibia Acoustic Sensor	Acoustic Sensor	1 MHz
Right and Left Shoulder Belt Tension	Belt Tension Load Cell	20 kHz
Lap Belt Tension	Belt Tension Load Cell	20 kHz
Head Acceleration SAE-X, Y, Z	Endevco 7264B-2000	20 kHz
Head Angular Rate SAE-Y	DTS ARS-12k	20 kHz
Right and Left 4th and 8th Ribs	CAE 06-062UW-350/P2	20 kHz
R and L Distal, Mid-shaft, and Proximal Anterior Femur	CAE 06-062UW-350/P2	20 kHz
Right Distal Tibia Bone Cell (4 strain gages)	CAE 06-062UW-350/P2	20 kHz
Right and Left Calcaneus	CAE 06-062UW-350/P2	20 kHz
R and L Ischial Tuberosities and Illiac Wings	CAE 06-062UW-350/P2	20 kHz

Additionally, piezoelectric acoustic (crack detection) sensors were placed on the shaft of each tibia using cyanoacrylate to be used for determining the onset of fracture. A proximity sensor attached to the side of the track was used to measure the incoming velocity of the hammer sled. The carriage sled was instrumented with Endevco 7270A-6000 (Meggitt Sensing Systems, San Juan Capistrano, CA) accelerometers on the z-axis of both the foot pan and seat pan to measure the input conditions of the test.

Data were sampled using two different data acquisition systems. Accelerometer and acoustic sensor data were sampled at 1 MHz using a Hi-Techniques Synergy high speed data acquisition system (Hi-Techniques, Madison, WI), while the remaining sensors were sampled at 20 kHz by a TDAS-Pro (Diversified Technical Systems, Seal Beach, CA) data acquisition system. High speed video footage was captured for each test using two Phantom cameras (Vision Research, Wayne, NJ) and two NAC Memrecam GX-1 cameras (NAC Image Technology, Charlotte, NC) operating at 2000 frames per second. Cameras were focused on both the seat and foot platens, while the others were used to capture lateral and overhead views of the carriage sled.

Pre-test CT and DEXA bone mineral density tests were performed to ensure no pre-existing fractures were present and that the bone mineral density fell within the normal range (T-score > -2.5) [29]. After instrumentation, an additional pre-test CT scan was performed to determine sensor location and ensure that application of instrumentation did not produce artifactual fracture. After each test, a post-test CT scan and necropsy were performed to determine the induced injuries.

The 50th percentile Hybrid-III ATD (Humanetics, Plymouth, MI) was instrumented with head, T1 and pelvis accelerometers in all axes, as well as angular rate sensors for measuring rotation about the Y-axis. A fully-instrumented Mil-LX was used as the lower leg on the right side and a fully-instrumented Hybrid-III leg was placed on the left. The use of two different ATD legs enabled both a comparison of the two leg designs under the same loading conditions, as well as enabled the data collected to be compared to existing lower extremity research, that also used different ATD legs.

Data Scaling

To eliminate anatomical variability in the data, the accelerations were scaled to a 50th percentile human male using the scaling technique described by Eppinger in 1984 [30]. This scaling technique enables the normalization of test data from various subject sizes to a standard 50th percentile male. For this study, the scaling factor based on the specimen mass and the scaled acceleration were calculated using the following equations:

$$\lambda_m = \frac{m_{50th\ percentile}}{m_{subject}} \tag{1}$$

where λ_m is the scaling factor and is the ratio of the mass of the 50th percentile male and the mass of the subject being scaled

$$a_{scaled} = \lambda_m^{-\frac{1}{3}} a_{subject} \tag{2}$$

where a_{scaled} and $a_{subject}$ are the scaled and subject accelerations

Tibia Force Calculation

An array of strain gages was used in place of an implantable tibia load cell to provide in-bone forces derived from the stress calculated at a cross-section of bone. Forces in this study were derived using a methodology similar to that used by Funk, et al. in 2006 [31]. However, the application of additional strain gages as well as the positioning of the strain gages allowed for a more accurate calculation of the force. Instead of being placed at the tibia mid-shaft, the strain gages were positioned at the distal tibia in order to decrease the bending contribution due to the curvature of the tibia, and to focus on the axial forces present in the distal tibia. Furthermore, the existence of additional strain gages enabled a more accurate determination of the neutral axis. An implantable load cell was not used for this application because of its tendency to produce artifactual injuries as well as alter the transmissibility of the leg.

Pre-test CT images of the tibia were used to determine the positions of the strain gages. These positions, in addition to the strain-time histories for each gage, were used to determine the position and orientation of the neutral axis for each time step. The average orientation angle of the neutral axis was calculated for the time prior to the peak strain of the first strain gage. This average orientation was used and the neutral axis was moved in order to make it pass through the geometric centroid of the tibia cross-section. The two strain gages furthest from the centroid on either side of the neutral axis were chosen to use in order to calculate the axial strain time history using Equation 3. Using this axial strain, Equation 4 relates the Young's modulus to strain rate based on McElhaney 1966 [32]. Using the cross-sectional area of the tibia calculated using Matlab and the CT images, the force-time history was calculated.

$$\varepsilon_{axial} = \varepsilon_i + \left(\varepsilon_j - \varepsilon_i\right) \frac{m_{N/A} x_i^g - y_i^g}{m_{N/A} x_i^g - y_i^g - m_{N/A} x_j^g + y_j^g} \quad (3)$$

In the above equation, ε_{axial} is the axial strain calculation, x^g and y^g are the positions of the strain gages in the cross-section, and $m_{N/A}$ is the slope of neutral axis.

$$E = 29.258(SR)^{0.0441} \quad (4)$$

where E is Young's modulus based on information from McElhaney [32] and Untaroiu [33], and SR is the strain rate.

III. RESULTS

While ODYSSEY was designed to replicate the underbody blast environment, the response of the Hybrid-III and the PMHS were expected to be significantly different. Care was taken to ensure that the acceleration pulses to the seat and foot platens were comparable for the matched-pair tests. Fig. 5 and Fig. 6 compare the seat and foot platen accelerations for the matched pair of tests (1.5 and 2.5), which demonstrates the ability to accurately produce repeatable boundary conditions for this test series.

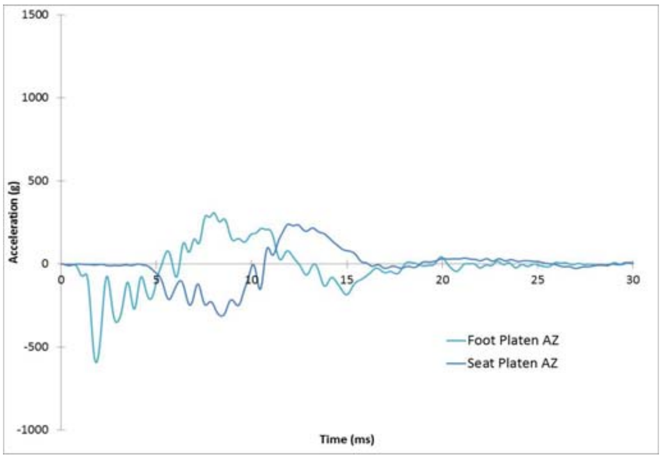

Fig. 5. Test 1.5 PMHS test seat and foot platen accelerations

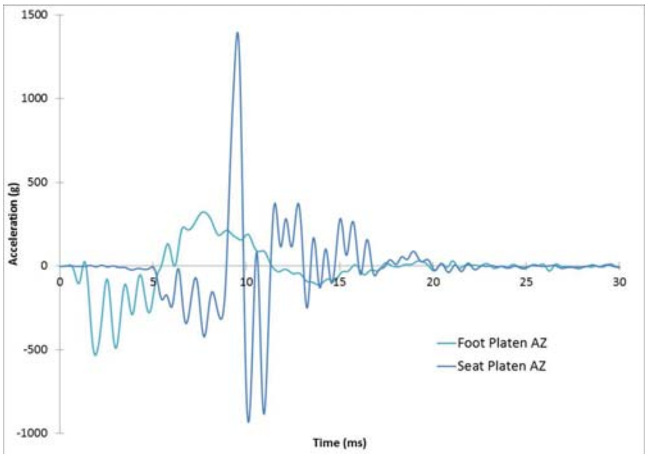

Fig. 6. Test 2.5 ATD test seat and foot platen accelerations

Table 6 provides a summary of results from both the PMHS and ATD tests. These results strongly reflect the stiffness of the Hybrid-III ATD in comparison to the human body as represented by the PMHS in this study and reinforces previous observations made about the lower extremities. Lower tibia force magnitudes as well as the tibia load rate suggest that the Mil-LX leg is a better representation of the human leg than the Hybrid-III under UBB loading conditions since, in many cases, the Hybrid-III load rate more than doubles that of the PMHS. The higher pelvis jerk in the Hybrid-III as compared to the PMHS demonstrates that the stiffness of the ATD could potentially affect how even the torso reacts under UBB loading. While previous research of this nature exists for the lower extremities, this is one of the first studies to compare the response of the ATD and PMHS to high rate SAE-Z loading.

TABLE 6
TEST RESULTS SUMMARY

<table>
<tr><th>Test ID</th><th colspan="2">Lower Tibia Peak Force
(N)</th><th colspan="2">Tibia Load Rate
(N/ms)</th><th>Tibia Axial Strain Rate
(µS/ms)</th><th>Max Axial Tibia Strain
(µS)</th><th>Avg. Pelvis Jerk
(g/ms)</th></tr>
<tr><td colspan="8">PMHS</td></tr>
<tr><td>1.1</td><td colspan="2">--</td><td colspan="2">--</td><td>1760.7</td><td>2992.9</td><td>--</td></tr>
<tr><td>1.2</td><td colspan="2">6280.0</td><td colspan="2">2317.6</td><td>2991.0</td><td>8752.5</td><td>320.7</td></tr>
<tr><td>1.3</td><td colspan="2">3310.0</td><td colspan="2">1106.3</td><td>1082.5</td><td>3770.1</td><td>260.9</td></tr>
<tr><td>1.4</td><td colspan="2">--</td><td colspan="2">--</td><td>1029.8</td><td>3499.3</td><td>16.4</td></tr>
<tr><td>1.5</td><td colspan="2">--</td><td colspan="2">--</td><td>2040.3</td><td>2841.1</td><td>204.4</td></tr>
<tr><td colspan="8">ATD</td></tr>
<tr><td></td><td>Mil-Lx</td><td>Hybrid-III</td><td>Mil-Lx</td><td>Hybrid-III</td><td></td><td></td><td></td></tr>
<tr><td>2.1</td><td>7775.3</td><td>14255.7</td><td>1775.1</td><td>4943.6</td><td>--</td><td>--</td><td>432.9</td></tr>
<tr><td>2.2</td><td>6459.3</td><td>14414.3</td><td>2057.5</td><td>5249.1</td><td>--</td><td>--</td><td>401.2</td></tr>
<tr><td>2.3</td><td>3770.5</td><td>6957.2</td><td>1022.9</td><td>2250.3</td><td>--</td><td>--</td><td>129.7</td></tr>
<tr><td>2.4</td><td>4332.7</td><td>7444.3</td><td>1194.8</td><td>2414.7</td><td>--</td><td>--</td><td>267.2</td></tr>
<tr><td>2.5</td><td>--</td><td>12589.2</td><td>--</td><td>4575.2</td><td>--</td><td>--</td><td>391.4</td></tr>
</table>

Board-certified radiologists analyzed each post-test CT scan to determine injuries sustained during testing. Additionally, orthopedic surgeons performed post-test necropsies to confirm these injuries as well as look for injuries that may have been unidentifiable via imaging. A summary of the injuries induced by these tests is shown in Table 7. When analyzing the injury data from these tests using only seat and foot platen acceleration as injury criteria, the pelvic structure appears to be the component that fails first when loaded in this scenario. Four out of the five tests produced serious pelvic fractures while only one out of the five tests produced significant lower extremity injuries.

TABLE 7
PMHS INJURY SUMMARY

Test	Lower Extremity Injuries	Pelvic Injuries	Other Injuries
1.1	R tibia plafond Fx, L calcaneus Fx, L 4th metatarsal Fx, R 4th metatarsal Fx	Bilateral Upper sacral alar Fx, Bilateral medial acetabulum Fx, R. Superior and Inferior Pubic Ramus Fx, Bilateral Ischial Tuberosity Fx	R. Clavicle, R. Scapula, R. 5th-7th Ribs (*Suggestion of mid and upper T-Spine anterior compression Fxs)
1.2	None	R. Sacral Alar Fx, Saggital Fx in mid to lower Sacrum, non-displaced Fx anterior/medial R. Acetabulum and lateral L. superior pubic ramus/acetabulum	Bilateral Clavicle, compression FX at T6, possible compression FX at T5, anterior wedge Fx at C7 -T4, R. 3rd rib
1.3	None	None	None
1.4	None	Non-displaced Fx of bilateral acetabulum and inferior pubic rami, sacral alar Fx	None
1.5	None	Comminuted bilateral superior/inferior pubic rami Fx	None

IV. DISCUSSION

Since a number of loading conditions were used in order to determine the thresholds of injury for the lower extremities and pelvis, only the subject responses for tests 1, 2 and 5 could be compared. For these tests, biofidelity corridors were developed for the Mil-LX, Hybrid-III and PMHS tibia acceleration for the z-axis. Fig. 7 shows how the Mil-LX, Hybrid-III and PMHS tibia acceleration corridors compare. The Mil-LX and PMHS tibia accelerations show reasonable agreement, though the Mil-LX tibia acceleration curve demonstrates oscillatory behavior due to its construction using damping elements. The Hybrid-III tibia acceleration exhibits a drastically different behavior, which is characteristic of its stiffness; the Hybrid-III acceleration spikes to a peak prior to both the PMHS and the Mil-LX. This spike is likely due to the stress wave traveling quickly through the rigid leg and then returning and slowly damping to an unnoticeable level where the global acceleration of the leg is dominant. These plots emphasize the need for compliant elements in the lower extremity to model the human more accurately. However, while this study shows good agreement between the PMHS and Mil-LX acceleration, room for improvement remains for the lower extremity design.

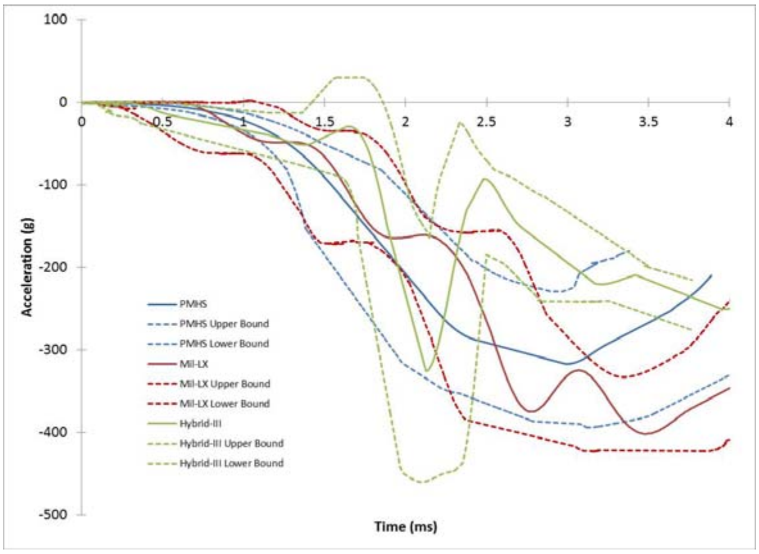

Fig. 7. Comparison of biofidelity corridors for z-axis mid-tibia acceleration.

Further examining the response of the lower extremities, a comparison of the lower tibia force provides supplemental proof of the Hybrid-III leg's inaccurate behavior under axial compression at higher loading rates. Fig. 8 and Fig. 9 show a comparison of the lower tibia load cell forces for the Mil-LX and Hybrid-III legs for the ATD test, and the force derived from the strain gages from the PMHS test. For both sets of tests, the PMHS and Mil-LX lower tibia forces have comparable magnitudes, while the Hybrid-III lower tibia force is more than double. Despite the agreement in magnitude, the Mil-LX and PMHS force plots have a discrepancy in the timing, particularly in the unloading from the peak force. The PMHS force relaxes faster than the Mil-LX force, which is likely due to the placement of the compliant structures in the Mil-LX. This characteristic of the PMHS tibia is not replicated by either of the ATD limbs tested. Thus, it is important that further research investigate the implications of such behavior on the development of ATDs to be used in this range of load rates.

The results from this test agree with the literature in regard to the stiffness of available ATD lower extremities in comparison to PMHS [34]. When comparing the force responses from the current study with those of past experiments, the same pattern of symmetric loading and unloading in the PMHS, but not the Mil-LX or Hybrid-III tibia, can be seen [34-35]. While these studies do not specifically investigate this phenomenon, the plots of their data confirm the behavior of the PMHS force, despite having used implantable load cells rather than a strain gage array to acquire tibia force.

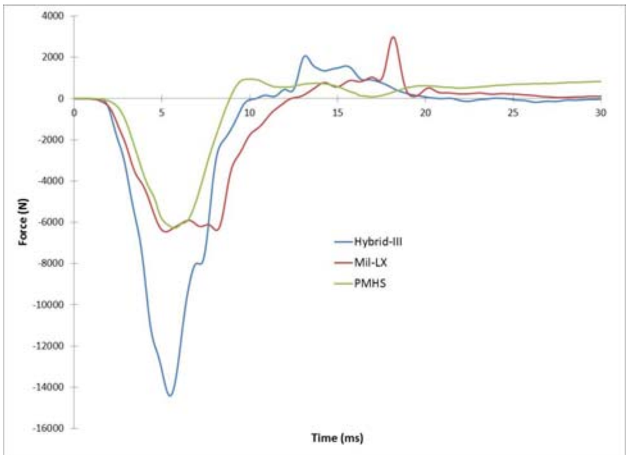

Fig. 8. Lower tibia z-axis force comparison for tests 1.2 and 2.2.

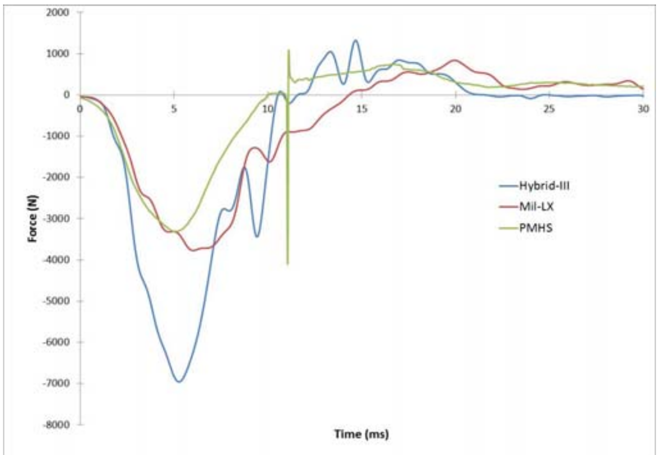

Fig. 9. Lower tibia z-axis force comparison for tests 1.3 and 2.3.

These tests provide valuable insight into the limitations of testing the Hybrid-III ATD in a vertical loading scenario. Fig. 10 and Fig. 11 show the acceleration response of the pelvis, T1 and head in the z-axis for both a PMHS and the Hybrid-III ATD. Test 1.3 was chosen for comparison due to the non-injurious nature of the test so as to avoid timing discrepancies attributable to energy dissipation through injury. Examination of these two plots highlights the overall stiff response of the Hybrid-III in comparison to the PMHS. The sharp rise to peak of the Hybrid-III pelvis acceleration is hardly analogous to the more gradual initial onset of acceleration in the PMHS pelvis due to the layer of flesh under the ischial tuberosities as well as due to compliance in the pelvis structure itself. Note also that because of the unrealistically stiff nature of the Hybrid-III, the T1 acceleration initiates prior to the pelvis acceleration, potentially due to the load from the foot platen (staged prior to the seat platen load) causing a rotation of the pelvis before the seat platen loading.

Further analysis reveals the differences in the shape of the T1 acceleration when comparing to the PMHS. Due to the differences between these curves, further attention was given to comparing the remaining tests, which showed similar results. One potential explanation for this disparity may be the difference in the kinematics of the two subjects. When studying the high speed video for these two tests, the Hybrid-III torso, perhaps again due to its structural rigidity, presented more of an x-component motion upon impact, whereas the PMHS exhibited more of a z-axis translation. This difference in the kinematics would also explain the differences in T1 and head z-axis acceleration magnitudes.

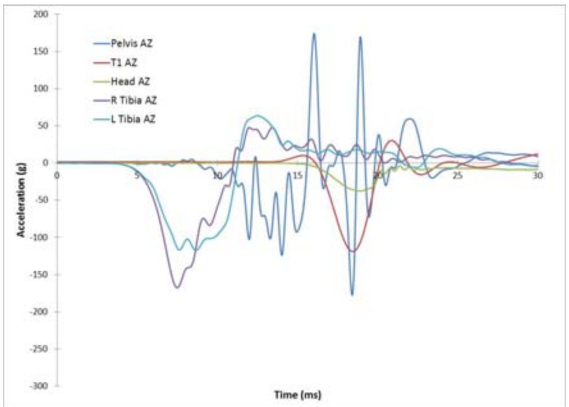

Fig. 10. PMHS z-axis acceleration response from test 1.3

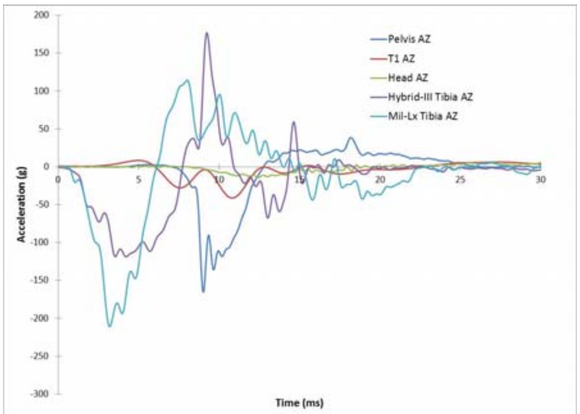

Fig. 11. Hybrid-III z-axis acceleration response from test 2.3

Due to the exploratory nature of this test series, a large range of seat and foot platen accelerations were tested and injury correlated to each of the input conditions. Despite the fact that the seat platen accelerations in tests 1.1 and 1.2 were somewhat larger than the range applicable to survivable UBB, and the foot platen accelerations were on the lower end of the UBB scale, a rough vertical injury threshold can be determined for both the lower extremity and pelvis. These data suggest the vertical injury threshold for the pelvis exists around 300g's of acceleration and 6.5 m/s peak velocity in 5 ms, while the threshold for the lower extremities lies in excess of 600 g's of acceleration and 10 m/s peak velocity in 4.5 ms.

The proposed preliminary threshold for the lower extremity agrees with results from Bir [34]; however, since little research exists for the response of the pelvis under high rate vertical loads, there is little to compare. Kargus, et al. performed a study on the effectiveness of seat design on injury probability using a 50th percentile Thor ATD (Humanetics, Plymouth, MI) dressed in personal protective equipment (PPE), and using the Dynamic Response Index to assess injury. This study showed that for vertical tests, injury was assessed in the Thor for a Δv (change in velocity) between 5.8 and 7.8 m/s [36]. The injury threshold for the pelvis developed from this study falls easily within this range. However, further work should investigate the effect of PPE on this injury threshold due to the effect of added inertia.

Limitations and Future Work

Due to the small number of PMHS involved in this test series as well as the variability of the test matrix, the data and conclusions from this test series must be considered preliminary until further statistical significance can be acquired through additional testing. However, the novelty of this test series provides unique insights into behavior of the human body under high rate vertical loads as well as invaluable information about the limitations of using the Hybrid-III ATD in a loading scenario for which it has not been validated. This research will serve as a steppingstone for future work on the kinematics of the human body and the ATD under UBB loads as well as will serve to provide a starting place for developing more accurate injury thresholds and injury criteria for the UBB loading environment.

V. CONCLUSIONS

Since this study consists of only five PMHS tests, the injury thresholds developed from this test series should be considered preliminary. However, the data collected from these tests provide insight into the response of the whole body under high rate loading conditions, which heretofore required the use of live-fire explosives in a less than ideal testing environment. Lower extremity force comparison between the ATD and PMHS reflect similar results to Bir, et al, but the novelty of the comparison for pelvis response limits the ability to compare to previous research [34]. The data collected from these matched-pair PMHS and ATD tests provide a useful metric from which to compare previous and future live-fire ATD test results to PMHS injury and kinematics data gathered from a controlled loading environment. The results from these tests are the first to relate the level and rate of load to the resulting injuries as well as to the matched ATD response in the first attempts at developing injury criteria for this new injury mechanism as well as highlight the inaccuracies associated with the use of existing ATDs in this loading environment.

VI. ACKNOWLEDGEMENT

The authors would like to thank the U.S. Department of Defense (Contract W81XWH-11-2-0086) and the U.S. Army Medical Research and Materiel Command and the U.S. Army Aeromedical Research Laboratory for their support of this research.

VII. REFERENCES

[1] Otte D, von Rheinbaben H, Zwiipp H, Biomechanics of injuries to the foot and ankle joint of car drivers and improvements for an optimal car floor development, Proceedings of the *Stapp Car Crash Conference,* 922514, 1992.

[2] Crandall et al., The influence of footwell intrusion on lower extremity response and injury in frontal crashes, *Annual Proceedings of the Association for the Advancement of Automotive* Medicine, 39:269-286, 1995.

[3] Kruger H, Heuser G, Kraemer B, Schmitz A, Foot loads and footwell intrusion in an offset frontal crash, *Proceedings of the 14th International Technical Conference on Enhanced Safety of* Vehicles, 94-S4-O-03, 1995.

[4] Crandall J, Kuppa S, Klopp G, Hall G, Pilkey W, Hurwitz S, Injury mechanics and criteria for the human foot and ankle under axial impacts to the foot, *International Journal of Crashworthiness*, 3(2):147-162, 1998.

[5] Yoganandan N, Pintar F, Kumaresan S, Boynton M, Axial impact biomechanics of the human foot-ankle complex, *Journal of Biomechanical Engineering*, 119(4):433-437, 1997.

[6] Funk J, Crandall J, Tourret L, MacMahon C, Bass C, Khaewpong K, Eppinger R, The axial injury tolerance of the human foot/ankle complex and the effect of Achilles tension, *Journal of Biomechanical Engineering*, 124:750-757, 2002.

[7] Wang, J, Bird, R, Swinton, B, Krstic, A, Protection of Lower Limbs Against Floor Impact in Army Vehicles Experiencing Landmine Explosion, *Journal of Battlefield Technology*, 4, 3, 2001.
[8] Ramasamy, A, Hill, A, Masouros, S, Gibb, J, Bull, A, & Clasper, J, Blast-reated Fracture Patterns: A Forensic Biomechanical Approach, *Journal of the Royal Society, 8*, pages 689-698, 2010.
[9] McKay, B, Development of Lower Extremity Injury Criteria and Biomechanical Surrogate to Evaluate Military Vehicle Occupant Injury During an Explosive Blast Event, Wayne State University Dissertation, 2010.
[10] Schueler, F, Mattern, R, Zeidler, F, Scheunert, D, Injuries of the Lower Legs—Foot, Ankle Joint, Tibia; Mechanisms, Tolerance Limits, Injury-Criteria Evaluation of a Recent Biomechanics Experiment-Series. *Proceedings of IRCOBI Conference*, Brunnen, Switzerland, pages 33-45, 1995.
[11] McKay, B, Bir, C, Lower Extremity Injury Criteria for Evaluating Military Vehicle Occupant Injury in Underbelly Blast Events. *Stapp Car Crash Journal*, 53, pages 229-249, 2009.
[12] Yoganandan, N, Pintar, F, Boynton, M, Begeman, P, Prasad, P, Kuppa, S, Dynamic Axial Tolerance of the Human Foot-Ankle Complex, *Proceedings of the 40th Stapp Car Crash* Conference, Albuquerque, New Mexico, pages 207-218, 1996.
[13] Kitagawa, Y, Ichikawa, H, Pal, C, Lower Leg Injuries Caused by Dynamic Axial Loading and Muscle Tensing, *Proceedings of the 16th International Technical Conference on the Enhanced Safety of* Vehicles, Windsor, Ontario, Canada, 1998.
[14] Quenneville, C, Fraser, G, Dunning, C, Development of an Apparatus to Produce Fractures from Short-Duration High-Impulse Loading with an Application in the Lower Leg, *Journal of Biomechanical* Engineering, 132, 1, 2010.
[15] Bass, C, Folk, B, Salzar, R, Davis, M, Harris, R, Rountree, M, Sanderson, E, Development of a Test Methodology to Evaluate Mine Protective Footwear, University of Virginia, Charlottesville, 2004.
[16] Gokcen, E, et al., Pelvic Fracture Mechanism of Injury in Vehicular Trauma Patients, *Journal of Trauma*, 36, 6, pages 789-796, 1994.
[17] Samaha, R, Elliott, D, NHTSA Side Impact Research: Motivation for Upgraded Test Proceedures, 18th International Technical Conference on the Enhanced Safety of Vehicles, Nagoya, Japan, 2003.
[18] States, J, States, D, Pathology and Pathogenesis of Injuries Caused by Lateral Impact Accidents, Paper 680773, *Society of Automotive Engineers (SAE)*, 1968.
[19] Grattan, E, Hobbs, J, Injuries to Hip Joint in Car Occupants, *British Medical Journal*, 1, 5636, pages 71-73, 1969.
[20] Schmidtke, S, Bidez, M, Alonso, J, Acetabular Fractures in Automotive Crashes: An Initial Report of 201 Patients, *International Conference on Pelvic and Lower Extremity* Injuries, 1995.
[21] Dakin, G, Eberhardt, A, Alonso, J, Stannard, J, Mann, K, Acetabular Fracture Patterns: Associations with Motor Vehicle Crash Information, *Journal of Trauma*, 47, 6, pages 1063-1071, 1999.
[22] Salzar, R, Genovese, D, Bass, C, Bolton, J, Guillemot, H, Damon, A, Crandall, J, Load Path Distribution within the Pelvic Structure Under Lateral Loading, *Journal of Crashworthiness*, 14, 1, pages 99-110, 2009.
[23] Guillemot, H, Besnault, B, Robin, S, Got, C, Coz, J, Lasaste, F, Pelvic Injuries in Side Impact Collisions: A Field Accident Analysis and Dynamic Tests on Isolated Pelvic Bones, *Stapp Car Crash Conference Proceedings*, Paper No. 973322, 1997.
[24] Salzar, R, et al., Development of Injury Criteria for Pelvic Fracture in Frontal Crashes, *Traffic Injury Prevention, 7, 3,* 2006.
[25] McCoy, G, Johnstone, R, Kenwright, J, Biomechanical Aspects of Pelvic and Hip Injuries in Road Traffic Accidents, *Journal of Orthopaedic Trauma*, 3, 2, pages 118-123, 1989.
[26] Pattimore, D, Ward, E, Thomas, P, Bradford, M, The Nature and Cause of Lower Limb Injuries in Car Crashes, *Stapp Car Crash Conference Proceedings,* Paper No. 912901, 1991.
[27] Dischinger, P, Cushing, B, Kerns, T, Injury Patterns Associated with Direction of Impact: Drivers Admittedto Trauma Centers, *Journal of Trauma*, 35, 3, pages 454-458, 1993.
[28] Siegel, J, et al, Safety Belt Restraints and Compartment Intrusions in Frontal and Lateral Motor Vehicle Crashes: Mechanisms of Injuries, Complications, and Acute Care Costs, *Journal of Trauma*, 34, 5, pages 736-758, 1993.
[29] Organization World Health. *WHO Scientific Group on the Prevention and Management of Osteoporosis*, Geneva: WHO Press, 2000.
[30] Eppinger, R, Marcus, J, Morgan, R, Development of Dummy and Injury Index for NHTSA's Thoracic Side Impact Protection Research Program, Warrendale, Pennsylvania: Society of Automotive Engineers, 1984.

[31] Funk, J, Crandall, J, Calculation of Tibial Loading using Strain Gages, Rocky Mountain Bioengineering Symposium and International ISA Biomedical Sciences Instrumentation Symposium, Terre Haute, Indiana, 2006.

[32] McElhaney, J.H., Dynamic Response of Bone and Muscle Tissue, *Journal of Applied Physiology*, 21, 4, pages 1231-1236, 1966.

[33] Untaroiu, C, Kerrigan, J, Kam, C, Crandall, J, Correlation of Strain and Loads Measured in the Long Bones with Observed Kinematics of the Lower Limb during Vehicle-Pedestrian Impacts, *Stapp Car Crash Journal*, 51, pages 433-467, 2007.

[34] Bir, C, Barbir, A, Dosquet, F, Wilhelm, M, van der Horst, M, Wolfe, G, Validation of Lower Limb Surrogates as Injury Assessment Tools in Floor Impacts Due to Anti-Vehicular Land Mines, *Military Medicine*, 173, 12, pages 1180-1184, 2008.

[35] Pandelani, T, Reinecke, D, Philippens, M, Dosquet, F, Beetge, F, The Practical Evaluation of the Mil-Lx Lower Leg when Subjected to Simulated Vehicle Under Belly Blast Load Conditions, 2010.

[36] Kargus, R, Li, T, Frydman, A, Nesta, J, Methodology for Establishing the Mine/IED Resistance Capacity of Vehicle Seats for Crew Protection, Army Research Lab Adelphi MD, 2008.